

much energy). In reionizing these primary products, their excess internal energy may produce unstable cations, but this may increase the cross section for anion formation by increasing the electron affinity. With such selection of experimental conditions this technique is useful for the structural characterization of  $C_4H_8^{*+}$  isomers from a variety of sources.

**Acknowledgment.** The authors thank R. F. Porter, B. Leyh, and F. Turecek for helpful discussions, and K. D. Henry for data processing. Generous financial support was provided by the

National Science Foundation and instrumentation by the National Institutes of Health.

**Registry No.** Cs, 7440-46-2; Na, 7440-23-5; Hg, 7439-97-6; 1- $C_4H_8$ , 106-98-9; 2- $C_4H_8$ , 107-01-7; *i*- $C_4H_8$ , 115-11-7; *c*- $C_6H_5CH_3$ , 594-11-6; *c*- $C_4H_8$ , 287-23-0; *n*-BuOH, 71-36-3; 1- $C_4H_8^{*+}$ , 34467-39-5; 2- $C_4H_8^{*+}$ , 34526-42-6; *i*- $C_4H_8^{*+}$ , 34526-44-8; *c*- $C_3H_5CH_3^{*+}$ , 56306-64-0; *c*- $C_4H_8^{*+}$ , 34474-99-2; benzene, 71-43-2;  $\beta$ -valerolactone, 15890-55-8; *n*-butyl acetate, 123-86-4; *sec*-butyl acetate, 105-46-4; isobutyl acetate, 110-19-0; *tert*-butyl acetate, 540-88-5;  $\gamma$ -valerolactone, 108-29-2; methylcyclopentane, 96-37-7; cyclohexane, 110-82-7.

## Product Kinetic Energy Release Distributions as a Probe of the Energetics and Mechanisms of Organometallic Reactions Involving the Formation of Metallacyclobutanes in the Gas Phase

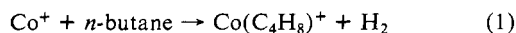
Petra A. M. van Koppen,<sup>†</sup> Denley B. Jacobson,<sup>†</sup> Andreas Illies,<sup>†,§</sup> Michael T. Bowers,<sup>\*,†</sup> Maureen Hanratty,<sup>†</sup> and J. L. Beauchamp<sup>\*,†</sup>

Contribution from the Department of Chemistry, University of California, Santa Barbara, California 93106, and Arthur Ames Noyes Laboratory of Chemical Physics,<sup>‡</sup> California Institute of Technology, Pasadena, California 91125. Received August 26, 1988

**Abstract:** Product kinetic energy release distributions and collision-induced dissociation studies are used to probe the energetics and mechanisms of several gas-phase organometallic reactions involving the formation of metallacyclobutanes. Reaction of atomic cobalt ions with 1-pentene yields  $Co(C_2H_4)^+$ . Loss of  $C_3H_6$  in this process exhibits a *bimodal* kinetic energy release distribution. The low-energy portion can be modeled using statistical phase space theory by assuming that propylene is eliminated. The high-energy portion of the distribution is similar to that observed for the decarbonylation of cyclobutanone by  $Co^+$  to yield  $Co(CO)^+$ . It is inferred for both systems that cyclopropane elimination is being observed with a tight transition state and a reverse activation energy. The characteristically broad kinetic energy release distributions cannot be described by statistical theories. Similar results are observed with  $Fe^+$  as a reactant. In this case, however, the reaction with 1-pentene leads to a broadened rather than a bimodal distribution. These arguments are substantiated using product distributions measured in collision-induced dissociation studies of various adducts which might have structures analogous to those invoked for the reactions of  $Co^+$  and  $Fe^+$  with cyclobutanone. Metastable loss of CO is also observed in these reactions. Fitting the statistical phase space theory to the measured distribution yields a heat of formation for the cobaltacyclobutane ion of  $274 \pm 5$  kcal/mol. The heat of formation (0 K) of the ferracyclobutane ion is less well determined but is approximately 268 kcal/mol. These are substantially higher (by 27 and 16 kcal/mol, respectively) than those for the corresponding isomeric propylene complexes. From these measurements, we estimate strain energies of cobaltacyclobutane and ferracyclobutane to be 22 and 18 kcal/mol, respectively, to be compared with 26 kcal/mol for cyclobutane.

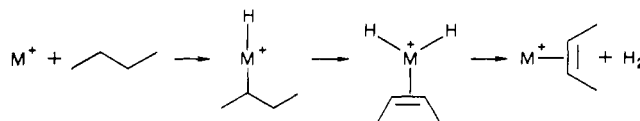
An intriguing aspect of transition metal-ion chemistry is the facility with which gas-phase atomic metal ions induce skeletal rearrangements of hydrocarbons.<sup>1-8</sup> For example, transition metal ions react exothermically with hydrocarbons to eliminate hydrogen, alkanes, or alkenes by processes which involve both bond cleavage and formation.

This is particularly apparent for the first-row transition metal ions  $Fe^+$ ,  $Co^+$ , and  $Ni^+$  where C-C bond cleavage and formation are pervasive. Elucidating the mechanism of these reactions has proven to be a challenge for the available experimental techniques for studying ionic processes in the gas phase. The dehydrogenation of *n*-butane, process 1, by  $Co^+$  represents an example. Initially,

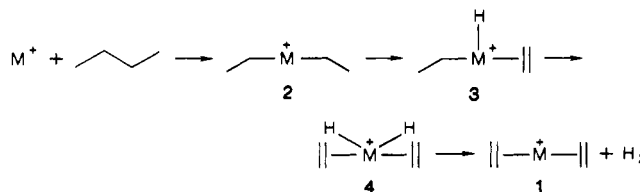


this reaction was believed to proceed by a simple C-H bond insertion followed by  $\beta$ -hydrogen elimination process as depicted in Scheme I.<sup>9</sup> Detailed structural studies on the product of

### Scheme I



### Scheme II



reaction 1, however, revealed that it comprises, not a 2-butene-metal ion complex, but rather a bisethylene complex **1**.<sup>10</sup> A

<sup>†</sup> University of California.

<sup>§</sup> Present address: Department of Chemistry, Auburn University, Auburn, AL 36849-5312.

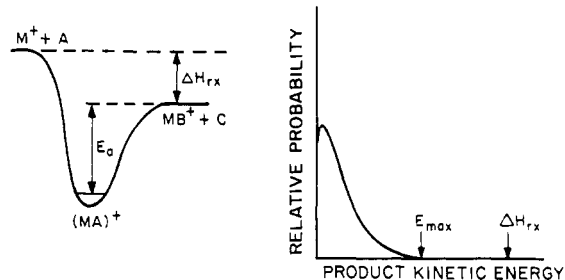
<sup>‡</sup> California Institute of Technology.

<sup>‡</sup> Contribution No. 7770.

(1) Byrd, G. D.; Freiser, B. S. *J. Am. Chem. Soc.* **1982**, *104*, 5944.

(2) Allison, J.; Freas, R. B.; Ridge, D. P. *J. Am. Chem. Soc.* **1979**, *101*, 1332.

(a) TYPE I (No Barrier for Reverse Association Reaction)



(b) TYPE II (Large Barrier for Reverse Association Reaction)

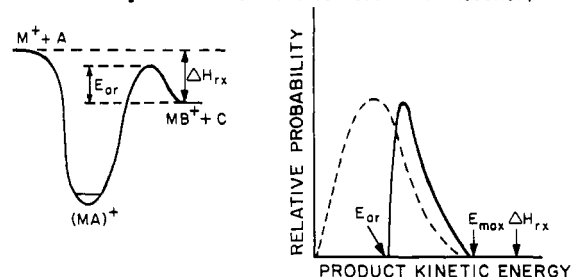
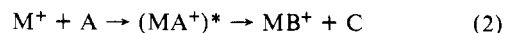


**Figure 1.** Two hypothetical potential energy surfaces for the reaction  $M^+ + A \rightarrow MB^+ + C$  and the corresponding product kinetic energy release distributions in the center-of-mass frame.

mechanism for formation of **1** is depicted in Scheme II and involves initial insertion into the internal C–C bond.<sup>11</sup> In addition, reaction with *n*-butane-1,1,1,3,3,3-*d*<sub>6</sub> yields substantial scrambling of the label, showing that intermediates **2** and **3** or intermediates **3** and **4** rapidly interconvert prior to dehydrogenation.<sup>5</sup>

Employing a variety of structural probes as well as specific isotopic labeling has provided insights relating to overall reaction mechanisms in addition to some specific details for the potential energy surfaces appropriate for the reaction of  $Fe^+$ ,  $Co^+$ , and  $Ni^+$  with simple hydrocarbons. Additional aspects of these reactions may be probed by monitoring kinetic energy release distributions for decomposition of nascent  $M^+ - A$  complexes ( $M$  = the metal ion, and  $A$  = the organic moiety). For example, we recently demonstrated that dehydrogenation of isobutane and *n*-butane by  $Co^+$  yields strikingly different kinetic energy release distributions, revealing differences in the dynamics of the exit channel (H–H bond formation process).<sup>12</sup> This type of specificity in reaction dynamics is unattainable using other structural probes as well as specific isotopic labeling studies.<sup>9</sup>

In a gas-phase bimolecular association reaction between  $M^+$  and  $A$  which involves a strong interaction such as bond formation, the association adduct  $(MA)^+$  may contain a large amount of internal excitation. In the absence of collision, the "chemically activated" complex  $(MA)^+*$  may utilize the excess internal energy for molecular rearrangement and subsequent fragmentation to yield one or more products (e.g., reaction 2).<sup>13</sup> It is possible to



measure the relative translational energies of the products  $MB^+$  and  $C$  as they separate using a reverse geometry double-focusing mass spectrometer. Any internal energy that is converted into translational energy during the dissociation will cause a spread in the energy of the product ions which is then detected by scanning the electrostatic analyzer.<sup>14</sup> Deconvolution of the peak shape yields a translational energy release distribution in the center-of-mass frame which can reveal details about the potential energy surface over which the dissociation occurs.<sup>15</sup>

Simplified reaction coordinate diagrams such as those presented in Figure 1 illustrate how the amount of energy appearing in product translation for a given dissociation reaction can reflect specific details of the potential energy surface. In Figure 1, the collision adduct  $MA^+$  containing internal energy  $E^*$  is depicted fragmenting to  $MB^+ + C$  along two hypothetical potential energy surfaces.<sup>16</sup> Statistical theories,<sup>16–18</sup> such as phase space theory,<sup>18c</sup> have been successful in modeling translational energy release distributions for reactions on a type I surface, where there is no barrier, excluding a centrifugal barrier,<sup>19</sup> for the reverse association reaction (Figure 1a). These theories predict a product translational energy distribution such as the one shown in the right-hand portion of Figure 1a. A decomposition in which the final step involves a substantial release of energy due to the presence of a reverse activation barrier almost always produces a kinetic energy release distribution which deviates substantially from that predicted by statistical theories. In such cases, it may be necessary to carry out more sophisticated trajectory calculations on model potential energy surfaces to reproduce the experimental kinetic energy releases. This has been feasible for only a limited number of systems<sup>20</sup> and will not be attempted here. The maximum kinetic energy which can be released is the reaction exothermicity,  $\Delta H_{rxn}$ .

For a dissociation process on a type I surface we have shown that the calculated kinetic energy release distributions are sensitive mainly to the reaction exothermicity and not to the choice of vibrational frequencies and structural parameters.<sup>12b</sup> Hence by fitting experimental and calculated distributions it is possible to extract the overall reaction thermochemistry and product ion heats of formation which are often unknown. For example, the loss of methane in the reaction of  $Co^+$  with isobutane yields a kinetic energy release distribution which can be fit with statistical phase space theory to give a heat of formation for the product ion  $Co(\text{propylene})^+$  of 247 kcal/mol. Reaction of  $Co^+$  with cyclopentane yields the same product ion with a similarly derived heat of formation of 247 kcal/mol at 0 K.<sup>12b</sup>

As shown in Figure 1b, a type II surface involves a barrier with activation energy ( $E_{ar}$ ) for the reverse association reaction. In the absence of coupling between the reaction coordinate and the other degrees of freedom after the transition state has been passed, all of the reverse activation energy will appear as translational energy of the separating fragments. The resulting translational

(13) Henschman, M. *Ion-Molecule Reactions*; Franklin, J. L., Ed.; Plenum Press: New York, 1972; p 101.

(14) Cooks, R. G.; Beynon, J. H.; Caprioli, R. M.; Lester, G. R. *Metastable Ions*; Elsevier: New York, 1973.

(15) Details in obtaining kinetic energy distributions and average kinetic energy are in: Jarrold, M. F.; Illies, A. J.; Kirchner, N. J.; Wagner-Redeker, W.; Bowers, M. T.; Mandich, M. L.; Beauchamp, J. L. *J. Phys. Chem.* **1983**, *87*, 2313.

(16) A more complete discussion may be found in: (a) Waage, E. V.; Rabinovitch, B. S. *Chem. Rev.* **1970**, *70*, 377. (b) Forst, W. *Theory of Unimolecular Reactions*; Academic Press: New York, 1973. (c) Robinson, P. J.; Holbrook, K. A. *Unimolecular Reactions*; Wiley: New York, 1972.

(17) Safran, S. A.; Weinstein, N. D.; Herschbach, D. R.; Tully, J. C. *Chem. Phys. Lett.* **1972**, *12*, 564.

(18) (a) Pechukas, P.; Light, J. C.; Rankin, C. J. *Chem. Phys.* **1966**, *44*, 794. (b) Nikitin, E. *Theor. Exp. Chem. (Engl. Trans.)* **1965**, *1*, 285. (c) Chesnavich, W. J.; Bowers, M. T. *J. Am. Chem. Soc.* **1976**, *98*, 8301. Chesnavich, W. J.; Bowers, M. T. *J. Chem. Phys.* **1978**, *68*, 901. Chesnavich, W. J.; Bowers, M. T. *Prog. React. Kinet.* **1982**, *11*, 137.

(19) For discussion, see: Su, T.; Bowers, M. T. In *Gas-Phase Ion Molecule Chemistry*; Bowers, M. T., Ed.; Academic Press: New York, 1979.

(20) See, for example: (a) Kato, S.; Morokuma, K. *J. Chem. Phys.* **1980**, *73*, 3900. (b) Santamaria, J.; Benito, R. M. *Chem. Phys. Lett.* **1984**, *109*, 478.

(3) (a) Burnier, R. C.; Byrd, G. D.; Freiser, B. S. *J. Am. Chem. Soc.* **1981**, *103*, 4360. (b) Burnier, R. C.; Byrd, G. D.; Freiser, B. S. *J. Am. Chem. Soc.* **1982**, *104*, 3565.

(4) Tolbert, M. A.; Beauchamp, J. L. *J. Am. Chem. Soc.* **1984**, *106*, 8177.

(5) (a) Houriet, R.; Halle, L. F.; Beauchamp, J. L. *Organometallics* **1983**, *2*, 1818. (b) Halle, L. F.; Armentrout, P. B.; Beauchamp, J. L. *Organometallics* **1982**, *1*, 963.

(6) (a) Armentrout, P. B.; Halle, L. F.; Beauchamp, J. L. *J. Am. Chem. Soc.* **1981**, *103*, 6624. (b) Armentrout, P. B.; Beauchamp, J. L. *J. Am. Chem. Soc.* **1981**, *103*, 6628.

(7) Jacobson, D. B.; Freiser, B. S. *Organometallics* **1984**, *4*, 513.

(8) Jacobson, D. B.; Freiser, B. S. *J. Am. Chem. Soc.* **1983**, *105*, 7492.

(9) Armentrout, P. B.; Beauchamp, J. L. *J. Am. Chem. Soc.* **1981**, *103*, 784.

(10) Jacobson, D. B.; Freiser, B. S. *J. Am. Chem. Soc.* **1983**, *105*, 5197.

(11) This mechanism was first proposed to explain the dehydrogenation of *n*-butane by  $Ni^+$ . See: Halle, L. F.; Houriet, R.; Kappes, M. M.; Staley, R. H.; Beauchamp, J. L. *J. Am. Chem. Soc.* **1982**, *104*, 6293.

(12) (a) Hanratty, M. A.; Beauchamp, J. L.; Illies, A. J.; Bowers, M. T. *J. Am. Chem. Soc.* **1985**, *107*, 1788. (b) Hanratty, M. A.; Beauchamp, J. L.; Illies, A. J.; van Koppen, P. A. M.; Bowers, M. T. *J. Am. Chem. Soc.* **1988**, *110*, 1.

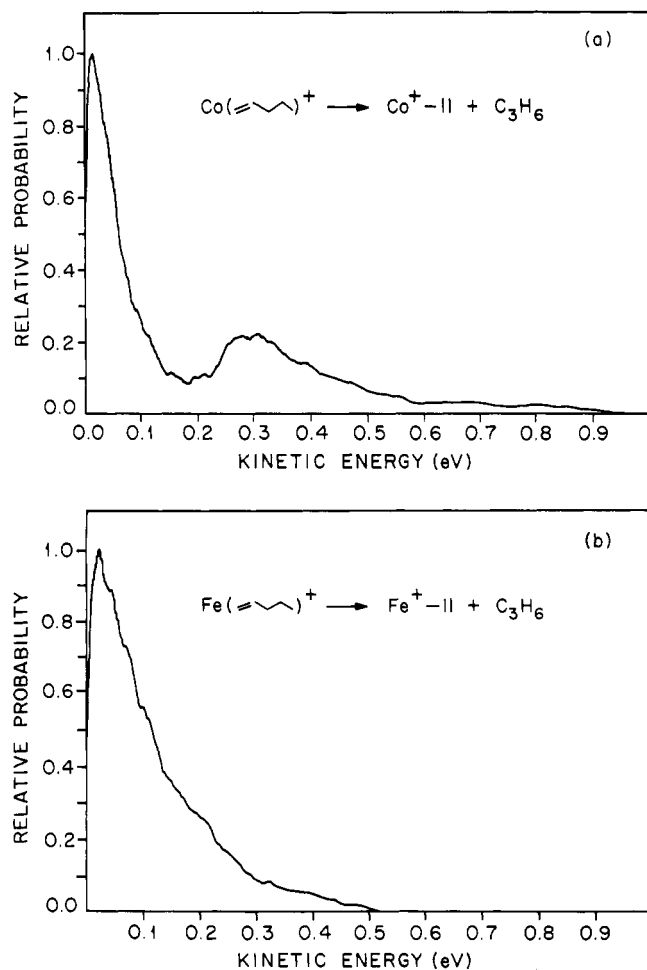


Figure 2. Kinetic energy release distributions for the loss of (a)  $C_3H_6$  from  $Co(1-pentene)^+$  and (b)  $C_3H_6$  from  $Fe(1-pentene)^+$ .

energy release is shifted from zero by the amount  $E_{ar}$  and may be peaked to higher kinetic energy due to angular momentum constraints.<sup>17,18</sup>

Even without a detailed knowledge of transition state structures and activation parameters, qualitative features of the potential energy surface can be deduced from the shape of the kinetic energy release distribution. For instance, the maximum energy release,  $E_{max}$ , places a lower limit on the reaction exothermicity regardless of the type of potential energy surface. Although the two cases in Figure 1 represent extremes, they are useful as models with which to interpret observed kinetic energy distributions. Frequently, exit channel effects<sup>21</sup> distort the translational energy of the products as they separate and shift the energy distribution to lower energies.<sup>22</sup> The amount of energy appearing as relative translation of the products will depend on the details of the potential energy surface and the dynamic effects which occur as the products separate. Nevertheless, the shape of the kinetic energy distribution and the maximum kinetic energy release often suggest which type of potential energy surface is the more appropriate description for the system.

The potential energy surfaces for the bimolecular reactions of metal ions with hydrocarbons and ketones are in general more complex than the above examples since they often involve a variety of products which result from multiple and perhaps interconnecting pathways. For example, the exothermic reactions of iron and cobalt ions with 1-pentene result in the elimination of  $H_2$ ,  $CH_4$ ,  $C_2H_4$ , and  $C_3H_6$  as important reaction pathways.<sup>6,23</sup> The kinetic

Table I. Metastable Product Distributions of  $Fe^+$  and  $Co^+$  Complexes with Cyclobutanone and 1-Pentene

	M = Fe	M = Co	
$M(\text{cyclobutanone})^+$	$MC_3H_6^+ + CO$	.85	.80
	$MCO^+ + C_3H_6$	.08	.18
	$M^+ + C_4H_8O$	.07	.02
$M(1-pentene)^+$	$MC_5H_8^+ + H_2$	.01	.02
	$MC_4H_6^+ + CH_4$	.03	.01
	$MC_3H_6^+ + C_2H_4$	.89	.95
	$MC_2H_4^+ + C_3H_6$	.07	.01
	$M^+ + C_5H_{10}$	.002	.01

energy release distribution for a given reaction channel, however, is characteristic primarily of the exit channel.

A major stimulus for the present study was provided by the observation of a very unusual bimodal kinetic energy release distribution for the loss of  $C_3H_6$  from chemically activated adduct of  $Co^+$  with 1-pentene (see Figure 2a). Although structure has been observed in kinetic energy release distributions of small ions,<sup>24</sup> such structure has always been due to internal state distributions of the products. In the case of  $Co^+(1-pentene)$  we felt the bimodal distribution could be due to competitive loss of  $C_3H_6$  as propene and cyclopropane from distinct reaction intermediates. In particular we felt decomposition of a metallacyclobutane intermediate might be responsible for the proposed cyclopropane elimination. Earlier work has shown decarbonylation of cyclic ketones yields metallacyclic butanes as reaction products.<sup>25</sup> Consequently, we chose to look at kinetic energy releases from reactions of  $Fe^+$  and  $Co^+$  with cyclobutanone. The results of these and related studies will be reported here and the implications of the results discussed.

### Experimental Section

Measurements of the metastable kinetic energy release distributions and collision-induced dissociation (CID) spectra were obtained using a reverse geometry double-focusing mass spectrometer (VG Instruments ZAB-2F<sup>26</sup>) with a temperature-variable ion source constructed at UCSB.<sup>24</sup> The iron and cobalt ions were formed by electron impact (150 eV) on  $Fe(CO)_5$  and  $Co(CO)_3NO$ , respectively. Typical source pressures were  $10^{-3}$  Torr, and source temperatures were generally kept below 270 K to minimize decomposition of the  $Fe(CO)_5$  or  $Co(CO)_3NO$  on insulating surfaces.

The organometallic ions were formed in the ion source under nearly field-free conditions to avoid translational excitation of the ions. Upon exiting the source, the ions were accelerated to 8 kV and mass analyzed. Metastable ions which decompose in the second field-free region between the magnetic and electric sectors were detected by scanning the voltage of the electric sector. The metastable peaks were accumulated in a multichannel analyzer and numerically differentiated to obtain the kinetic energy release distributions.<sup>24</sup> The energy resolution was such that the main beam did not contribute significantly to the metastable peak widths.

In some cases artifact peaks were observed. These artifacts are thought to be due to first field-free region metastables or collisions with lenses and deflection of energetic neutrals into the electron multiplier.<sup>27</sup> When possible, deuterium-labeled compounds were used to minimize interference of artifact peaks with the true metastable peaks.

A collision cell located at the focal point between the magnet and electric sectors was used to obtain collision-induced dissociation (CID) spectra with helium (collision gas) admitted until a 50% main beam attenuation was observed. Natural metastables were separated out from the CID spectra by applying -750 V to the collision cell.<sup>28</sup> Fragment

(21) See, for example: Farrar, J. M.; Lee, Y. T. *J. Chem. Phys.* **1976**, *65*, 1414, and discussion of results in; Marcus, R. A. *J. Chem. Phys.* **1975**, *62*, 1372. Worry, G.; Marcus, R. A. *J. Chem. Phys.* **1977**, *67*, 1636.

(22) Sudbo, S. A.; Schulz, P. A.; Shen, Y. R.; Lee, Y. T. *J. Chem. Phys.* **1978**, *63*, 2312.

(23) Jacobson, D. B.; Freiser, B. S. *J. Am. Chem. Soc.* **1983**, *105*, 7484.

(24) (a) Jarrold, M. F.; Illies, A. J.; Bowers, M. T. *Chem. Phys.* **1982**, *65*, 19. (b) Kirchner, N. J.; Bowers, M. T. *J. Phys. Chem.* **1987**, *91*, 2573.

(25) Halle, L. F.; Crowe, W. E.; Armentrout, P. B.; Beauchamp, J. L. *Organometallics* **1984**, *3*, 1694.

(26) Morgan, R. P.; Beynon, J. H.; Bateman, R. H.; Green, B. N. *Int. J. Mass Spectrom. Ion Phys.* **1978**, *28*, 171.

(27) Ast, T.; Bozorgzaden, M. H.; Wiebers, J. L.; Beynon, J. H.; Brenton, A. G. *Org. Mass Spectrom.* **1979**, *14*, 313.

(28) Beynon, J. H.; Cooks, R. G. *Int. J. Mass Spectrom. Ion Phys.* **1976**, *19*, 107.

**Table II.** Experimental Average Kinetic Energy Release for Exothermic Reactions of  $M = \text{Co}^+$  and  $\text{Fe}^+$ 

	$\bar{E}_t$ , eV		
	M = Co	M = Fe	
$M(\text{cyclobutanone})^+$	$M^+ \text{C}_3\text{H}_6 + \text{CO}$	.12	.15
	$M^+ \text{CO} + \text{C}_3\text{H}_6$	.32	.23
	$M^+ \text{C}_3\text{H}_6 + \text{CO}^a$		
	$M^+ + \text{C}_3\text{H}_6$	.041	.047
$M(\text{1-pentene})^+$	$\text{MC}_2\text{H}_4^+ + \text{C}_3\text{H}_6$	.23 <sup>b</sup>	.12
	$\text{MC}_3\text{H}_6^+ + \text{C}_2\text{H}_4$	.061	.066

<sup>a</sup>Loss of CO in the ion source. <sup>b</sup>Bimodal (see discussion in text).

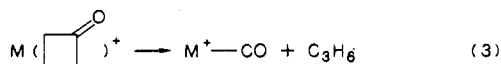
ions formed by CID in the biased collision cell will be shifted in energy by an amount equal to  $(m_2/m_1)V$ , where  $V$  is the applied potential and  $m_1$  and  $m_2$  are the precursor and fragment ion masses, respectively.<sup>28-30</sup>

All chemicals were obtained commercially in high purity and used as supplied except for multiple freeze-pump-thaw cycles to remove non-condensable gases.

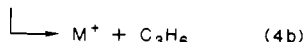
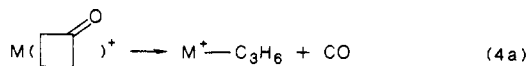
## Results

Metastable decomposition reactions of nascent  $\text{Fe}^+$  and  $\text{Co}^+$  complexes with cyclobutanone and 1-pentene were studied.<sup>31</sup> The observed product distributions are presented in Table I.

The average kinetic energy releases,  $\bar{E}_t$ , for selected metastable decompositions are given in Table II. The average kinetic energy releases for  $\text{Fe}^+$  and  $\text{Co}^+$  are similar for most reactions. Note that the average kinetic energy release observed for the loss of  $\text{C}_3\text{H}_6$  for reaction 3 is relatively large in comparison to the average



kinetic energy release for the loss of  $\text{C}_3\text{H}_6$  for reaction 4b.



Reaction 4a occurs in the ion source followed by reaction 4b in the second field-free region.

Although the average kinetic energy release gives some indication of the amount of energy appearing in product translation, it is more informative to examine the shape of the entire distribution. For example, elimination of  $\text{C}_3\text{H}_6$  from nascent  $\text{Co}(\text{1-pentene})^+$  yields an unusual *bimodal* distribution (Figure 2a), suggesting two distinct decomposition processes. In contrast a much narrower kinetic energy release distribution is observed for the loss of  $\text{C}_3\text{H}_6$  from  $\text{Fe}(\text{1-pentene})^+$  (Figure 2b). Loss of  $\text{C}_2\text{H}_4$  from  $\text{Fe}(\text{1-pentene})^+$  and  $\text{Co}(\text{1-pentene})^+$  produce relatively narrow distributions that are virtually identical.

Statistical phase space theory<sup>18</sup> is used to model the experimental kinetic energy distributions. The calculations have been

(29) Okuno, K. *Mass Spectrosc.* 1976, 24, 107.

(30) Wachs, T.; Van de Sande, C. C.; McLafferty, F. W. *Org. Mass Spectrom.* 1976, 11, 1308.

(31) One complicating factor should be considered. In addition to  $\text{MA}^+$  adducts formed in the source via bimolecular  $M^+ + A$  association reactions, ligand displacement reactions can also sometimes yield  $\text{MA}^+$  complexes with sufficient energy to decompose further (i.e.,  $\text{MCO}^+ + A \rightarrow \text{MA}^+ + \text{CO}$ ). The adduct resulting from ligand displacement, however, should contain much less excess energy than the association adduct and should be relatively stable to decomposition as a metastable process.<sup>32</sup> The effect of ligand displacement reactions may be more extensive in the collision-induced dissociation spectra since CID preferentially samples the more stable, longer lived species.

(32) Freas, R. B.; Ridge, D. P. *J. Am. Chem. Soc.* 1980, 102, 7129.

**Table III.** Reaction Enthalpies and Experimental and Theoretical Average Kinetic Energy Release for Reactions of  $\text{Co}^+$  and  $\text{Fe}^+$ 

	$\bar{E}_t$ (eV)		
	$-\Delta H^a$	Expt	Theory <sup>b</sup>
$\text{Fe}^+ + \text{cyclobutanone} \longrightarrow \text{Fe}^+(\text{cyclobutanone}) + \text{CO}$	0.51	0.15	0.10
$\text{Co}^+ + \text{cyclobutanone} \longrightarrow \text{Co}^+(\text{cyclobutanone}) + \text{CO}$	0.59	0.12	0.11
$\text{Fe}^+ + \text{cyclobutanone} \longrightarrow \text{Fe}^+ \text{CO} + \triangle$	0.72	0.23	0.10
$\text{Co}^+ + \text{cyclobutanone} \longrightarrow \text{Co}^+ \text{CO} + \triangle$	0.94	0.32	0.12
$\text{Fe}^+ + \text{1-pentene} \longrightarrow \text{Fe}^+ \text{CO} + \text{C}_3\text{H}_6$	0.66 <sup>c</sup> (0.29) <sup>c</sup>	0.12	0.071 <sup>c</sup>
$\text{Co}^+ + \text{1-pentene} \longrightarrow \text{Co}^+ \text{CO} + \text{C}_3\text{H}_6$	0.96 <sup>c</sup> (0.59) <sup>c</sup>	0.23 <sup>d</sup>	0.085 <sup>c</sup>
$\text{Fe}^+ + \text{1-pentene} \longrightarrow \text{Fe}^+ \text{CO} + \text{C}_2\text{H}_4$	0.73		0.082
$\text{Fe}^+ + \text{1-pentene} \longrightarrow \text{Fe}^+(\text{cyclobutanone}) + \text{C}_2\text{H}_4$	0.05	0.072	0.041
$\text{Co}^+ + \text{1-pentene} \longrightarrow \text{Co}^+ \text{CO} + \text{C}_2\text{H}_4$	1.05		0.097
$\text{Co}^+ + \text{1-pentene} \longrightarrow \text{Co}^+(\text{cyclobutanone}) + \text{C}_2\text{H}_4$	0.02	0.061	0.027

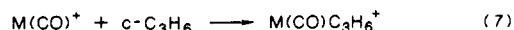
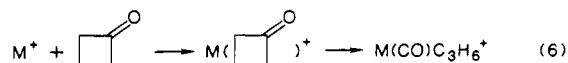
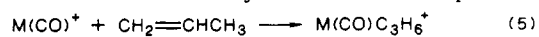
<sup>a</sup>Heat of reaction in eV at 0 K. <sup>b</sup>Statistical phase space theory using the methods outlined in ref 18c. <sup>c</sup>Assuming the propene structure for the  $\text{C}_3\text{H}_6$  product neutral. The number in parentheses is for cyclopropane product. <sup>d</sup>Bimodal (see discussion in text).

previously described.<sup>12b</sup> The main purpose of the calculations is to determine whether a statistical model, which assumes a type I surface and equipartitioning of the excess energy, is adequate to describe the experimental energy release distribution. Parameters used in the phase space theory calculations are summarized in Appendix A.

The kinetic energy release distributions for nearly all the systems studied were modeled using phase space theory assuming a type I surface. Theoretical and experimental average kinetic energy releases,  $\bar{E}_t$ , are presented in Table III. For the loss of CO from  $\text{Co}(\text{cyclobutanone})^+$  and  $\text{Fe}(\text{cyclobutanone})^+$  fairly good agreement was found in both cases between the theoretical and experimental results suggesting a statistical kinetic energy release.

The theoretically predicted kinetic energy release distributions for  $\text{C}_3\text{H}_6$  loss from  $\text{Co}(\text{cyclobutanone})^+$  and  $\text{Fe}(\text{cyclobutanone})^+$ , however, are much narrower than the experimentally observed distributions. The average kinetic energy release was calculated to be 0.10 eV and experimentally observed to be 0.23 eV for the Fe system. The corresponding numbers are 0.12 and 0.32 eV, respectively, for the Co system. The results of these calculations clearly indicate that these systems cannot be modeled by assuming a purely statistical energy release from a type I potential energy surface.

The collision-induced decomposition spectra (CID) of isomeric  $\text{M}(\text{C}_4\text{H}_6\text{O})^+$  and  $\text{M}(\text{C}_3\text{H}_6)^+$  complexes are presented in Tables IV and V for cobalt and iron. The  $\text{M}(\text{C}_4\text{H}_6\text{O})^+$  reactant ion was formed via reactions 5–7. The objective here is to compare the



CID spectrum of  $\text{M}(\text{CO})\text{C}_3\text{H}_6^+$  produced in reaction 6 to those produced in reactions 5 and 7. The CID spectrum of  $\text{M}(\text{CO})\text{C}_3\text{H}_6^+$  produced in reaction 6 resembles that of  $\text{M}(\text{CO})$ -

**Table IV.** Collision-Induced Dissociation Spectra of  $MC_4H_6O^+$  Ions Formed from Reaction of  $MCO^+$  with Propene and Cyclopropane and  $M^+$  with Cyclobutanone

reactant neutral	fragment ions <sup>a,b</sup>													
	CoC <sub>3</sub> H <sub>6</sub>	CoC <sub>3</sub> H <sub>5</sub>	CoC <sub>3</sub> H <sub>4</sub>	CoC <sub>3</sub> H <sub>3</sub>	CoCO	CoC <sub>2</sub> H <sub>2</sub>	CoC <sub>2</sub> H	CoCH <sub>3</sub>	CoCH <sub>2</sub>	CoCH/CoC <sup>c</sup>	CoH	Co	C <sub>3</sub> H <sub>6</sub> /C <sub>3</sub> H <sub>5</sub> <sup>c</sup>	C <sub>3</sub> H <sub>3</sub>
propene	65	4.8	2.2	3.7	11.2	4.4	1.1	3.3	2.4	1.9	trace	b	0.4	0.5
cyclobutanone	37.8	5.4	2.0	2.8	33.8	1.0		5.5	10.1	3.2		b	1.4	0.7
cyclopropane	51.7	4.2	2.0	4.4	20.2	3.1	1.2	2.9	9.3	2.1	trace	b	0.4	0.8

reactant neutral	fragment ions <sup>a,b</sup>													
	FeC <sub>3</sub> H <sub>6</sub>	FeC <sub>3</sub> H <sub>5</sub>	FeC <sub>3</sub> H <sub>4</sub>	FeC <sub>3</sub> H <sub>3</sub>	FeCO	FeC <sub>2</sub> H <sub>2</sub> /FeC <sub>2</sub> H <sup>c</sup>	FeCH <sub>3</sub>	FeCH <sub>2</sub>	FeCH/FeC <sup>c</sup>	FeH	Fe	C <sub>3</sub> H <sub>6</sub> /C <sub>3</sub> H <sub>5</sub> <sup>c</sup>	C <sub>3</sub> H <sub>3</sub>	
propene	71.0	5.2		3.7	8.0	3.6	3.0	3.3	2.4	trace	b	0.4	0.2	
cyclobutanone	55.4	3.0		2.6	12.5	5.5	trace	21.5	2.6	trace	b	2.1	1.2	
cyclopropane	57.5	2.3		4.7	11.0	2.5	1.61	5.8	3.6	3.1	b	0.2	0.4	

<sup>a</sup>All values normalized to  $\sum I_i$ , excluding  $Co^+$  and  $Fe^+$  as fragment ions. <sup>b</sup> $I_i/\sum I_i$  ( $Fe^+, Co^+$ ) was 25% for propene and cyclopropane and 40% for cyclobutanone. The larger percentage for the cyclobutanone is most likely due to the adduct  $M(\text{cyclobutanone})^+$  rather than the  $(OC-M-C_3H_6)^+$  complex. Excluding the bare metal ion in comparing the  $MC_4H_6O^+$  CID spectra reflects more truly the decomposition of  $OC-M-C_3H_6^+$  without significant contribution from the adduct  $M(\text{cyclobutanone})^+$ . <sup>c</sup>These peaks could not be resolved in the CID spectra. The numbers reported are consequently representative of the sum of these intensities.

**Table V.** Collision-Induced Dissociation Spectra of  $MC_3H_6^+$  Ions

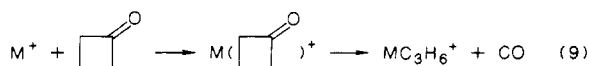
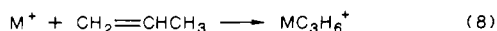
reactant neutral	fragment ions																
	Co-C <sub>3</sub> H <sub>5</sub>	Co-C <sub>3</sub> H <sub>4</sub>	Co-C <sub>3</sub> H <sub>3</sub>	Co-C <sub>3</sub> H <sub>2</sub>	Co-C <sub>3</sub> H	Co-C <sub>2</sub> H <sub>3</sub>	Co-C <sub>2</sub> H <sub>2</sub>	Co-C <sub>2</sub> H	Co-CH <sub>3</sub>	Co-CH <sub>2</sub>	CoCH	CoC	CoH	Co	C <sub>3</sub> H <sub>6</sub>	C <sub>3</sub> H <sub>5</sub>	C <sub>3</sub> H <sub>3</sub>
propene	1.2	1.2	3.1	2.1	0.8	0.9	3.6	2.2	3.8	2.8	1.4	1.1	trace	73.7	0.4	0.4	1.3
cyclobutanone	0.9	1.4	2.2	1.4	0.7	0.6	2.9	1.6	2.3	9.8	2.1	1.7	trace	70.2	0.3	0.4	0.8
cyclopropane	0.8	1.4	2.9	2.2	0.9	0.6	3.4	1.6	3.6	8.4	1.7	1.5	trace	70.0	0.2	0.4	1.0

reactant neutral	fragment ions																
	Fe-C <sub>3</sub> H <sub>5</sub>	Fe-C <sub>3</sub> H <sub>4</sub>	Fe-C <sub>3</sub> H <sub>3</sub>	Fe-C <sub>3</sub> H <sub>2</sub>	Fe-C <sub>3</sub> H	Fe-C <sub>2</sub> H <sub>3</sub>	Fe-C <sub>2</sub> H <sub>2</sub>	Fe-C <sub>2</sub> H	FeCH <sub>3</sub>	FeCH <sub>2</sub>	FeCH	FeC	FeH	Fe	C <sub>3</sub> H <sub>6</sub>	C <sub>3</sub> H <sub>5</sub>	C <sub>3</sub> H <sub>3</sub>
propene	0.8	0.5	3.9	1.1	0.6	1.0	1.6	2.9	3.1	3.0	1.6	3.0		73.6	0.3	0.5	0.9
cyclobutanone	0.4	0.3	2.6	0.8	0.5	0.6	1.2	1.5	1.5	29.6	5.1	3.0		47.7	trace	trace	0.5
cyclopropane	0.3	0.3	3.6	1.2	0.6	0.7	1.4	1.8	2.0	27.1	4.5	2.4		48.8	0.3	0.2	0.7

$(c-C_3H_6)^+$  more closely than that of  $M(CO)(CH_2=CHCH_3)^+$ , especially when comparing the relative product ion intensities of  $MCH_2^+$ ,  $MC_3H_6^+$ , and  $MCO^+$ .

CID spectra of  $MC_3H_6^+$  isomers are summarized in Table V. The  $MC_3H_6^+$  reactant ion was formed by the reactions 8–10. The

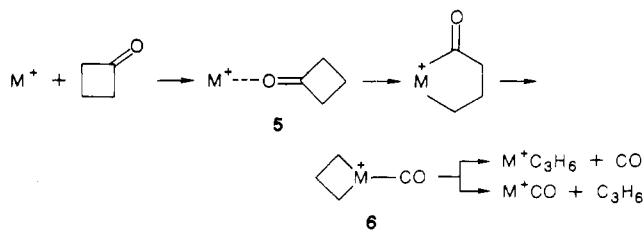


CID spectrum of  $FeC_3H_6^+$  formed via reaction 9 resembles that of  $FeC_3H_6^+$  formed from cyclopropane neutral rather than from propene neutral (compare  $FeCH_2^+$  and  $Fe^+$  product ion intensities). In the cobalt system these differences are much less substantial.

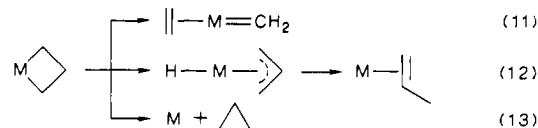
## Discussion

**Cyclobutanone.** Reactions of  $Fe^+$  and  $Co^+$  with cyclobutanone studied were loss of CO, reaction 4a, and loss of  $C_3H_6$ , reaction 3. A mechanism for formation of the products in reactions 3 and 4a is illustrated in Scheme III. Initially an activated complex, **5**, is formed between the metal ion and cyclobutanone followed by insertion into an  $\alpha$ -C-C bond. Carbonyl abstraction then occurs with competitive elimination of CO and  $C_3H_6$ . Consistent with this mechanism is the mechanism proposed for  $Co^+$  reacting with acetone.<sup>12b,33</sup> Scheme III suggests that  $M(CO)C_3H_6^+$  ions are initially formed as metallacyclobutane ions.<sup>33</sup> Beauchamp et al.<sup>34</sup>

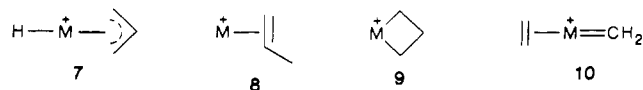
## Scheme III



have postulated metallacyclic species as intermediates in gas-phase organometallic reactions. Metallacyclobutanes rearrange and decompose in solution by three basic routes,<sup>33,35–37</sup> eq 11–13. By



analogy, we consider four possible structures for the  $MC_3H_6^+$  ions formed in reaction 4a: a  $\pi$ -allyl hydrido complex, **7**, a propene metal ion complex, **8**, a metallacyclobutane, **9**, and a carbene ethene complex, **10**.



(33) For a review of metallacyclobutane chemistry, see: Grubbs, R. H. *Comprehensive Organometallic Chemistry*, Wilkinson, G., Ed.; Pergamon Press: Oxford, England, 1982; Vol. 8, p 533.

(34) (a) Armentrout, P. B.; Beauchamp, J. L. *J. Chem. Phys.* **1981**, *74*, 2819. (b) Armentrout, P. B.; Beauchamp, J. L. *J. Am. Chem. Soc.* **1981**, *103*, 6628. (c) Stevens, A. E.; Beauchamp, J. L. *J. Am. Chem. Soc.* **1979**, *101*, 6449.

(35) Schrock, R. R. *Acc. Chem. Res.* **1979**, *12*, 98.

(36) Cushman, B. M.; Brown, D. B. *J. Organomet. Chem.* **1978**, *152*, C42.

(37) (a) Ephritikhine, M.; Green, M. L. H.; Mackenzie, R. E. *J. Chem. Soc., Chem. Commun.* **1976**, 619. (b) Adams, G. J. A.; Davies, S. G.; Ford, K. A.; Ephritikhine, M.; Todd, P. F.; Green, M. L. H. *J. Mol. Catal.* **1980**, *8*, 15.

In an attempt to determine the structure of the  $M(\text{CO})\text{C}_3\text{H}_6^+$  intermediate (proposed to be a metallacyclobutane complex in Scheme III), the collision-induced dissociation spectrum of this ion is compared to that of  $M(\text{CO})(\text{CH}_2=\text{CHCH}_3)^+$  and  $M(\text{CO})(\text{c-C}_3\text{H}_6)^+$  (Table IV). The CID spectrum of  $M(\text{CO})\text{C}_3\text{H}_6^+$  (6) resembles that of  $M(\text{CO})(\text{c-C}_3\text{H}_6)^+$  more than that of  $M(\text{CO})(\text{CH}_2=\text{CHCH}_3)^+$ , especially when comparing the relative product ion intensities of  $\text{MCH}_2^+$ . Thus, with the CO ligand present the metallacyclobutane does not appear to rearrange. This supports the contention that the  $\text{MC}_3\text{H}_6^+$  product ion and  $\text{C}_3\text{H}_6$  product neutral in reactions 4a and 3 correspond to a metallacyclobutane and cyclopropane, respectively.

The kinetic energy release distribution observed for CO elimination, reaction 4a, was relatively narrow for both  $\text{Fe}^+$  and  $\text{Co}^+$ . This contrasts with the broader distribution observed for  $\text{C}_3\text{H}_6$  elimination, reaction 3, for both  $\text{Co}^+$  and  $\text{Fe}^+$ . The kinetic energy release distributions for both reactions were modeled by theoretical phase space calculations. Three of the four possible structures (8, 9, and 10) were considered for the  $\text{MC}_3\text{H}_6^+$  product ion in reaction 4a. Fairly good agreement is found in comparing the experimental distribution with the theoretical distribution assuming the metallacyclobutane structure 9 for the  $\text{MC}_3\text{H}_6^+$  product ion as shown in Figure 3, a and b. These results yield heats of formation (at 0 K) of 274 and 268 kcal/mol, respectively, for the cobalta- and ferracyclobutanes. These heats of formation are 27 and 16 kcal/mol higher, respectively, than those of the isomeric propylene complexes. The calculated kinetic energy distribution was much broader than the experimental distribution using the metal-propene structure, 8, and somewhat narrower for the methyldene-ethene structure, 10.<sup>38</sup>

In calculating the kinetic energy release distributions, the only unknown which can dramatically affect the results is the metal-ligand bond energy for metal-propene, metallacyclobutane, or the carbene-ethene ion. As noted above, we have previously determined the cobalt-propene bond energy to be  $D^{\circ}_0 = 44 \pm 5$  kcal/mol.<sup>12b</sup> In order to fit the experimental distribution assuming the cobalt-propene structure, the bond energy would have to be lowered to 20 kcal/mol which would be unreasonable. Calculations assuming the  $\pi$ -allyl hydrido structure as the product ion were not carried out since the carbonyl metallacyclobutane does not appear to rearrange in this way. Experimental data can be fit with either the metallacyclobutane or the carbene-ethene structure. A somewhat better fit is obtained for the metallacyclic structure, but these data alone cannot be used to unambiguously distinguish between these two structures. However, FTMS results indicate no evidence for the iron carbene ethene ion.<sup>7</sup> Thus the metallacyclobutane structure 9 is most likely the product ion in reaction 4a.

A definite high-energy tail is observed experimentally for the iron system which is not reproduced theoretically (Figure 3b). The theoretical distributions for all three  $\text{FeC}_3\text{H}_6^+$  structures go to zero before the experimental distribution tails off to zero. A high-energy tail in the distribution is not completely surprising, however, since the actual potential surfaces for these reactions are more complex than the simple type I surface used in modeling these systems. The high-energy tail in the experimental distribution may be due to a rate-limiting barrier along the reaction coordinate in the step preceding the exit channel, such that energy randomization is not complete before the system goes out to products.

The calculated and experimental kinetic energy release distributions for the second reaction channel (3), loss of  $\text{C}_3\text{H}_6$  from

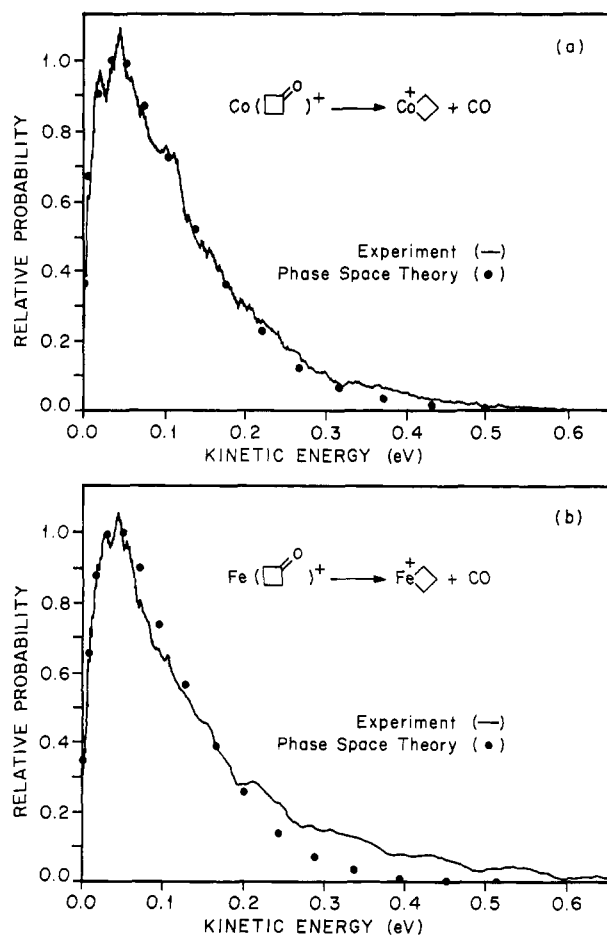


Figure 3. Experimental and theoretical kinetic energy release distributions for loss of (a) CO from  $\text{Co}(\text{cyclobutanone})^+$  and (b) CO from  $\text{Fe}(\text{cyclobutanone})^+$ .

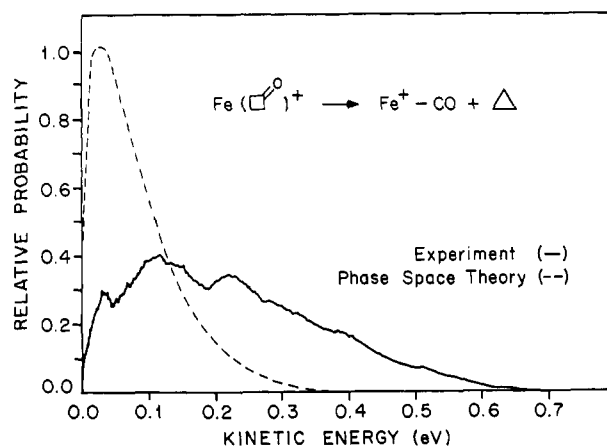


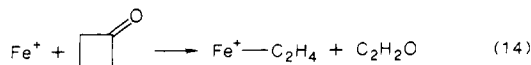
Figure 4. Experimental and theoretical kinetic energy release distributions for the loss of  $\text{C}_3\text{H}_6$  from  $\text{Fe}(\text{cyclobutanone})^+$ .

$\text{Fe}(\text{cyclobutanone})^+$ , are compared in Figure 4. As can be seen, the experimental distribution is much broader than that expected for a type I surface. The overall shape of the distribution for  $\text{C}_3\text{H}_6$  elimination suggests a type II surface with significant coupling in the exit channel which cannot be modeled by simple statistical theories. If a metallacyclobutane is the final intermediate prior to decomposition, as proposed in Scheme III, then cyclopropane would probably be the neutral  $\text{C}_3\text{H}_6$  product. A barrier in the exit channel is more likely for cyclopropane elimination than for the loss of propene since both bond cleavage and formation are occurring at the transition state in producing cyclopropane, whereas elimination of propene involves simple rupture of a donor-acceptor bond.

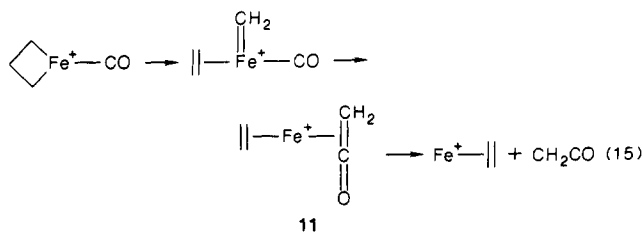
(38) An upper limit to the binding energy of trimethylene to  $\text{Fe}^+$  was found to be 97 kcal/mol by: Jacobson, D. B.; Freiser, B. S., *J. Am. Chem. Soc.* **1985**, *107*, 72. The corresponding binding energy from our calculations is 84 kcal/mol. This is calculated using the heats of formation  $\Delta H_f^{\circ}(\text{cyclopropane}) = 12.74$  kcal/mol from: Rosenstock, H. M.; Draxl, K.; Steiner, B. W.; Herron, J. T. *J. Phys. Chem. Ref. Data* **1977**, Suppl. 6, and  $\Delta H_f^{\circ}(\text{trimethylene}) = 72.2$  kcal/mol from: Doering, W. von E. *Proc. Natl. Acad. Sci. U.S.A.* **1981**, *78*, 5279.  $D^{\circ}_{298}(\text{ferracyclobutane}) = 24.7$  kcal/mol decomposing to  $\text{Fe}^+$  and cyclopropane. The estimated heats of formation for the metal carbene ethylene species are 282 and 283 kcal/mol for iron and cobalt, respectively.

In summary, the CID results, along with the kinetic energy release data and results from previous studies,<sup>34</sup> indicate that the proposed intermediate is the metallacyclobutane structure **5** which decomposes to yield cyclopropane rather than propene as the neutral product.

For iron an additional reaction with cyclobutanone involving C<sub>2</sub>H<sub>2</sub>O loss, reaction 14, is seen in bimolecular studies as a minor

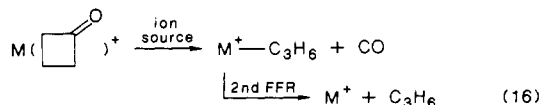


process.<sup>7</sup> Elimination of C<sub>3</sub>H<sub>6</sub> or C<sub>2</sub>H<sub>2</sub>O for Fe(cyclobutanone)<sup>+</sup>, reactions 3 and 14, cannot be distinguished in the present study. However, ketene elimination should occur from an ethene complex, **11**, which involves simple bond cleavage, process 15.

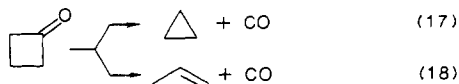


In addition, elimination of C<sub>2</sub>H<sub>2</sub>O as ketene is ~3 kcal/mol less exothermic than for cyclopropane elimination.<sup>38</sup> The lower exothermicity combined with simple bond cleavage in the exit channel should yield a *narrow* kinetic energy release for elimination of ketene from **11**. Thus, if both elimination of C<sub>3</sub>H<sub>6</sub> and C<sub>2</sub>H<sub>2</sub>O were occurring, then the kinetic energy distribution should have a bimodal appearance. Since this is not the case, the metastable elimination of mass 42 from Fe(cyclobutanone)<sup>+</sup> is believed to involve mainly loss of C<sub>3</sub>H<sub>6</sub>.

Reaction 4a occurs in the ion source as well as the second field-free region. The MC<sub>3</sub>H<sub>6</sub><sup>+</sup> product ion can be extracted from the source and the subsequent metastable loss of C<sub>3</sub>H<sub>6</sub> can then be studied (eq 16). Of interest here is the structure of the



decomposing MC<sub>3</sub>H<sub>6</sub><sup>+</sup> ion as well as the C<sub>3</sub>H<sub>6</sub> product neutral. In this case the average kinetic energy releases were small for both Co and Fe, and the overall shape of the distributions appear statistical in nature. These results indicate that the lowest energy transition state responsible for the metastable reaction is the same for cobalt and iron and that it is most likely the metal-propene structure. Phase space calculations were not done for these reactions since the internal energy of the MC<sub>3</sub>H<sub>6</sub><sup>+</sup> reactant ion is not clearly defined. The overall reaction thermochemistry for the formation of cyclopropane and propylene is identical with that for decomposition of cyclobutanone alone. Reaction 17 is en-



dothermic by 9.4 kcal/mol while process 18 is nearly thermo-neutral ( $\Delta H^\circ_0 = 0.8$  kcal/mol). The substantial endothermicity of reaction 17 guarantees that only propylene is being eliminated in the metastable decomposition reactions.

Further information is available from the CID spectra (Table V). The spectrum of FeC<sub>3</sub>H<sub>6</sub><sup>+</sup> ions produced in the source via reaction 16 resembles that of Fe(c-C<sub>3</sub>H<sub>6</sub>)<sup>+</sup> rather than that of Fe(CH<sub>2</sub>=CHCH<sub>3</sub>)<sup>+</sup> (compare the FeCH<sub>2</sub><sup>+</sup> and Fe<sup>+</sup> fragment ion intensities). In the cobalt system, the differences in the three CID spectra are smaller, indicating at least some isomerization to a common structure is taking place. The CoC<sub>3</sub>H<sub>6</sub><sup>+</sup> ions formed via reaction 16 compare more favorably in their reactivity to Co(c-C<sub>3</sub>H<sub>6</sub>)<sup>+</sup> than Co(CH<sub>2</sub>=CHCH<sub>3</sub>)<sup>+</sup>, however. These results suggest the metallacyclobutane structure **9** is initially formed for both Fe<sup>+</sup>

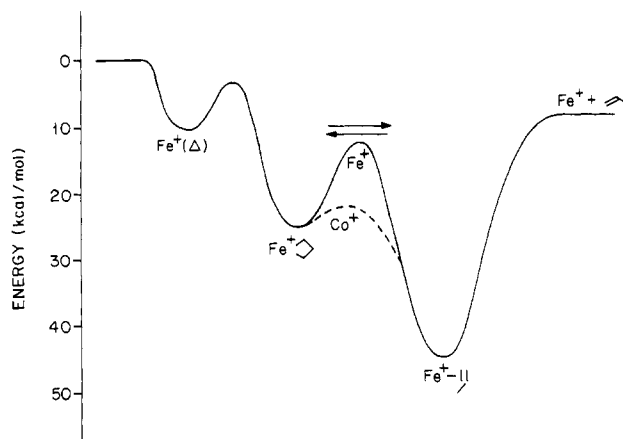
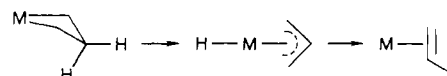


**Figure 5.** Qualitative potential energy diagram for the reaction  $\text{Fe}^+ + \text{c-C}_3\text{H}_6 \rightarrow \text{Fe}^+ + \text{CH}_2=\text{CHCH}_3$ . The relative energies of the structures shown are fairly well established although the barrier heights between them are not known. The surface for  $\text{Co}^+$  is similar with the exception of the lower barrier shown by the dotted line (see text for discussion).

#### Scheme IV



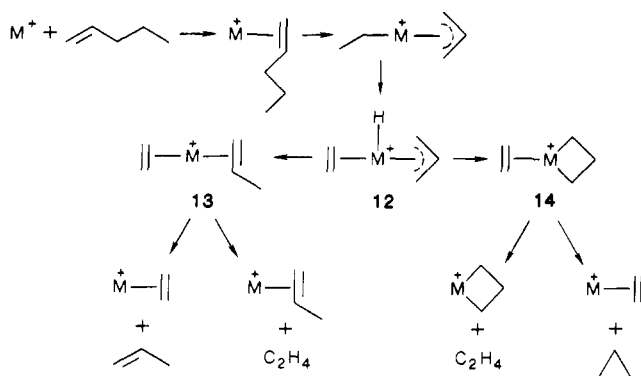
and  $\text{Co}^+$  systems by decarbonylation of cyclobutanone, and that isomerization is more extensive with  $\text{Co}^+$  than it is for  $\text{Fe}^+$ . Jacobson and Freiser came to the same conclusion in a previous study using an FTMS instrument,<sup>7,39</sup> which included both ligand exchange reactions and CID results. Peake, Gross, and Ridge<sup>40</sup> have presented CID spectra of  $\text{FeC}_3\text{H}_6^+$  product ions for a variety of olefin reactants, including cyclopropane and propene. These results are in good agreement with our findings (small differences are due to the fact that natural metastables are separated out from the CID spectra in our results). In their analysis, however, they conclude iron reacts with cyclopropane to initially form the ferracyclobutane but that it rearranges to the  $\text{C}_2\text{H}_4\text{Fe}^+=\text{CH}_2$  structure prior to collisional activation. They suggest this rearrangement occurs because loss of C<sub>2</sub>H<sub>4</sub> to form  $\text{Fe}^+=\text{CH}_2$  is a major process. The fact that  $\text{Fe}^+=\text{CH}_2$  is the largest fragment ion in the CID spectrum does not necessarily indicate that a rearrangement to the higher energy  $\text{C}_2\text{H}_4\text{Fe}^+=\text{CH}_2$  ion takes place *prior* to collisional activation. Since the ferracyclobutane structure was found to be stable on the millisecond time scale by Jacobson and Freiser,<sup>7</sup> it is probably the stable structure on the microsecond time scale as well, and hence is sampled in both our experiment and that of Peake et al.<sup>40</sup>

Summarizing, metal-propene structures are observed for both iron and cobalt in the metastable ion kinetic energy spectra, while metallacyclobutane structures are observed in the collisional activation spectra although some cobaltacyclobutane isomerizes to cobalt propene. These results are rationalized by the potential energy diagram shown in Figure 5. If the barrier to rearrangement from the metallacyclobutane structure to the metal-propene structure is below the metal-propene dissociation limit for both iron and cobalt, then those metallacyclobutane ions with enough energy to dissociate will rearrange to metal-propene prior to dissociation. Consequently, the kinetic energy release distributions would be the same for iron and cobalt. Collision-induced dissociation of the  $\text{M}^+\text{C}_3\text{H}_6$  ions, however, samples the stable ions at the bottom of the well. Thus, based on the CID product distributions, the barrier for rearrangement of ferracyclobutane to iron-propene must be substantially larger than for cobaltacyclobutane to cobalt-propene; i.e., there must be enough energy in the system to surmount the barrier to rearrangement in the cobalt case prior to collisional activation.

(39) Jacobson, D. B.; Freiser, B. S. *J. Am. Chem. Soc.* **1985**, *107*, 72.

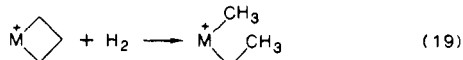
(40) Peake, D. A.; Gross, M. L.; Ridge, D. P. *J. Am. Chem. Soc.* **1984**, *106*, 4307.

## Scheme V



The degree of puckering of the metallacyclobutane ring is believed to be important in rearrangement of the metallacyclobutane species to a propene-metal species.<sup>3a</sup> A  $\pi$ -allyl hydrido intermediate is formed in the rearrangement process, Scheme IV. The greater the puckering the more favorable the H-atom transfer becomes. Our results suggest the possibility that the ferracyclobutane ion may be nearly planar while the cobaltacyclobutane ion may have significant puckering.

Based on the heats of formation determined for cobaltacyclobutane and ferracyclobutane ions in this study, the enthalpy change for reaction 19 is estimated to be 4 and 8 kcal/mol less exothermic,

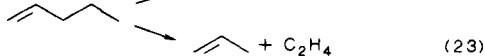
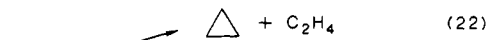


respectively, than for the analogous processes involving cyclobutane.<sup>41</sup> Using the accepted strain energy of 26 kcal/mol for cyclobutane,<sup>42</sup> this yields estimated strain energies of 22 kcal/mol for cobaltacyclobutane and 18 kcal/mol for ferracyclobutane. These values are comparable to the strain energy of thoracyclobutane,<sup>43</sup> similarly estimated to be 17 kcal/mol for bis(permethylocyclopentadienyl)-3,3-dimethylthoracyclobutane. Based on the ease with which four-membered platinacycloalkane rings are formed, it has been suggested that ring strain in species such as bis(triethylphosphine)-3,3-dimethylplatinacyclobutane is small compared to that in cyclobutane.<sup>44</sup> The present results clearly show that this conclusion, based on indirect reaction kinetic arguments rather than direct thermodynamic measurements, is certainly not a general one. *While not as large as those of cyclobutane, strain energies of metallacyclobutanes are substantial.*

**1-Pentene.** The studied reactions of  $\text{Fe}^+$  and  $\text{Co}^+$  with 1-pentene were loss of  $\text{C}_3\text{H}_6$  (reaction 20) and loss of  $\text{C}_2\text{H}_4$  (reaction 21).



Further decomposition of  $\text{MC}_2\text{H}_4^+$  or  $\text{MC}_3\text{H}_6^+$  was not observed, consistent with the substantial endothermicity associated with the formation of ethene and  $\text{C}_3\text{H}_6$  (cyclopropane or propene) from 1-pentene, (reactions 22 and 23), for which  $\Delta H^\circ_0 = 28.4$  and 19.8 kcal/mol, respectively).



The bimodal kinetic energy release distribution observed for  $\text{C}_3\text{H}_6$  elimination in the reaction of  $\text{Co}^+$  with 1-pentene (Figure

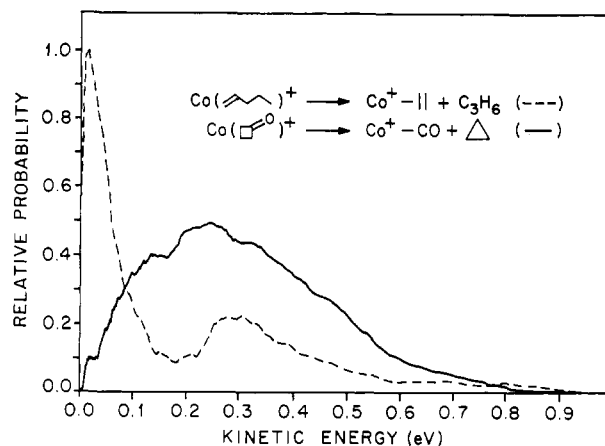


**Figure 6.** Kinetic energy release distribution for the loss of cyclopropane from  $\text{Co}(\text{cyclobutanone})^+$  (arbitrarily normalized to 0.5) superimposed on  $\text{C}_3\text{H}_6$  loss from  $\text{Co}(1\text{-pentene})^+$ .

2a) indicates two reaction pathways are available. The low-energy component with maximum probability near zero suggests a reaction which occurs along a type I surface. In fact, it is very similar to the energy release associated with ethene elimination from  $\text{Co}(1\text{-pentene})^+$ . A mechanism consistent with these observations is illustrated in Scheme V.<sup>2a,35</sup> Initially, the metal inserts into the allylic C-C bond generating an alkyl  $\pi$ -allyl complex. This is followed by  $\beta$ -hydrogen elimination generating the hydrido-allyl complex, 12, which is the key intermediate in this mechanism. Once 12 is formed  $\text{C}_2\text{H}_4$  and  $\text{C}_3\text{H}_6$  are eliminated via 13 and 14 as shown.

Loss of propene from the bis-olefin structure is expected to occur without a reverse activation barrier and is probably responsible for the low-energy release. Loss of cyclopropane from the cobaltacyclobutane intermediate 14 is probably responsible for the high-energy component. This suggestion is supported by the results for cyclopropane elimination from  $\text{Co}(\text{cyclobutanone})^+$ . The kinetic energy release distribution for cyclopropane elimination from  $\text{Co}(\text{cyclobutanone})^+$  and from  $\text{Co}(1\text{-pentene})^+$  should be comparable since the final decomposing structures, 15 and 16,



and product ions,  $\text{CoCO}^+$  and  $\text{CoC}_2\text{H}_4^+$ , are similar in many respects. Comparing the high-energy component of the bimodal distribution for cyclopropane elimination from  $\text{Co}(1\text{-pentene})^+$  to the kinetic energy release distribution for the loss of cyclopropane from  $\text{Co}(\text{cyclobutanone})^+$ , Figure 6, it is apparent that both the peak maxima and peak shapes are very similar. The similarity is somewhat surprising since the exothermicity for the reactions differ by 0.3 eV. We believe, however, that the kinetic energy release distribution reflects more directly the barrier in the exit channel rather than the available energy. These results support the contention that the high-energy component in the kinetic energy release distribution for  $\text{C}_3\text{H}_6$  elimination from  $\text{Co}(1\text{-pentene})^+$  is, in fact, cyclopropane. Conversion from the metallacyclobutane intermediate 6 to the bis-olefin structure 5 would simply lead to the low-energy kinetic energy release component.

The kinetic energy release distribution for  $\text{C}_3\text{H}_6$  elimination from  $\text{Fe}(1\text{-pentene})^+$  is not bimodal, but it is broader than expected in comparison to  $\text{C}_2\text{H}_4$  elimination; the average kinetic energy releases are 0.12 and 0.066 eV for the loss of  $\text{C}_3\text{H}_6$  and  $\text{C}_2\text{H}_4$ , respectively. The phase space calculation for propene elimination from  $\text{Fe}(1\text{-pentene})^+$  also predicts a narrower kinetic energy release distribution relative to the experimental distribution, as shown in Figure 7. Loss of cyclopropane from the ferracyclobutane intermediate could be responsible for the broadening in the distribution. This suggestion is supported by the results for the loss of cyclopropane from  $\text{Fe}(\text{cyclobutanone})^+$ . As was discussed for

(41) Heats of formation of the methyl ethyl metal ions are estimated from earlier results for dimethyl metal ions<sup>12b</sup> using group equivalents.

(42) Wiberg, K. B. *Angew. Chem., Int. Ed. Engl.* 1986, 25, 312.

(43) Fredrick, C. M.; Marks, T. J. *J. Am. Chem. Soc.* 1986, 108, 425.

(44) Moore, S. S.; DiCosimo, R.; Sowinski, A. F.; Whitesides, G. M. *J. Am. Chem. Soc.* 1981, 103, 948.



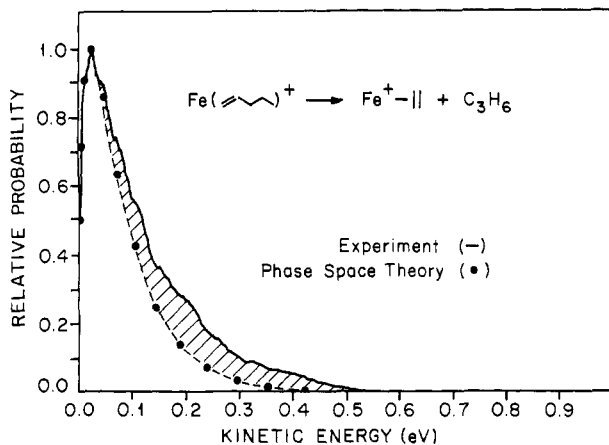


Figure 7. Experimental and theoretical kinetic energy release distributions for the loss of  $C_3H_6$  from  $Fe(1-pentene)^+$ . The propene structure is assumed for the  $C_3H_6$  product neutral in the calculation.

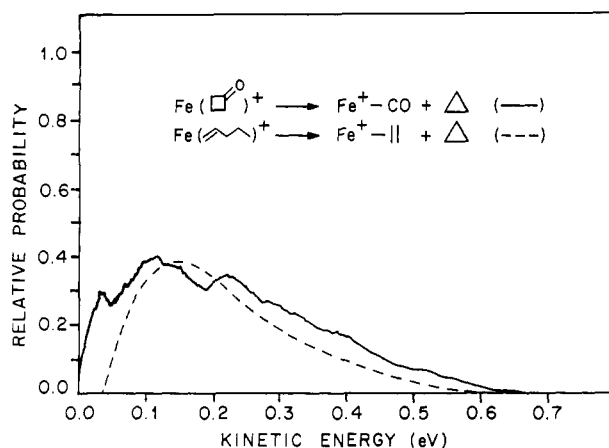


Figure 8. The cross-hatched area in Figure 7 abstracted, normalized, and superimposed on the kinetic energy release distribution for  $C_3H_6$  loss from  $Fe(cyclobutanone)^+$ .

the cobalt system, one would expect the kinetic energy release distribution for cyclopropane elimination from  $Fe(cyclobutanone)^+$  and  $Fe(1-pentene)^+$  to be very nearly the same since the final decomposing structures, **17** and **18**, and product ions,  $OC-Fe^+$



and  $C_2H_4-Fe^+$  are similar. Thus, one would expect the peak maximum to be approximately the same for cyclopropane elimination from both  $Fe(cyclobutanone)^+$  and  $Fe(1-pentene)^+$ . For the  $Fe(cyclobutanone)^+$  system the maximum is  $\sim 0.1$  eV. Hence one would not expect to be able to resolve the loss of cyclopropane from loss of propene. As a result, a single broad distribution rather than a bimodal distribution is observed. The cross-hatched area in Figure 7 represents the difference between experimental and theoretical kinetic energy release distributions for  $C_3H_6$  loss from  $Fe(1-pentene)^+$ . This difference abstracted, normalized, and super-imposed on the kinetic energy release distribution for  $C_3H_6$  loss from  $Fe(cyclobutanone)^+$  is presented in Figure 8. The overlap of the two distributions is quite good, especially in view of the fact that dissociation of **18** to yield cyclopropane is 0.4 eV less exothermic than in the case of **17**. This result further supports a mechanism in which both propene and cyclopropane are eliminated (Scheme V).

In calculating the kinetic energy release distribution for  $C_2H_4$  elimination from  $Fe(1-pentene)^+$  and  $Co(1-pentene)^+$ , both the metal-propene and metallacyclobutane structures were considered as possible product ions. The calculated kinetic energy distribution was broader than the experimental distribution when the  $M^+-$

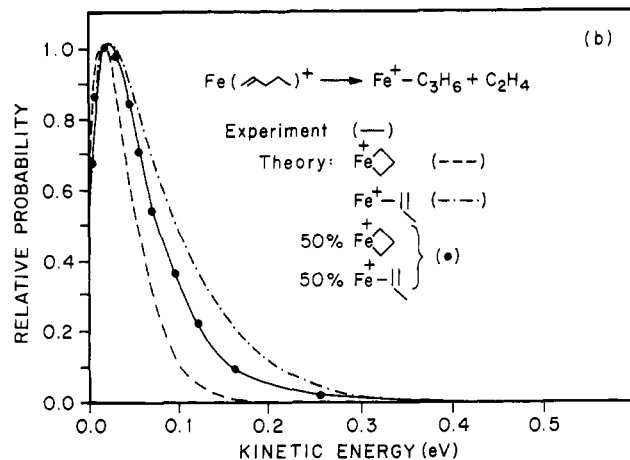
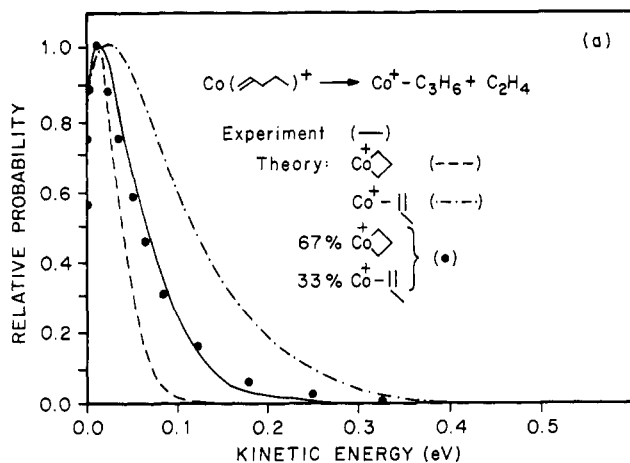


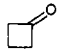
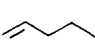
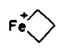
Figure 9. Experimental and theoretical kinetic energy release distributions for loss of (a)  $C_2H_4$  from  $Co(1-pentene)^+$  and (b)  $C_2H_4$  from  $Fe(1-pentene)^+$ . In each case three theoretical kinetic energy distributions are given. The distributions assuming  $M^+-propene$  product are significantly broader than experiment in both systems. The distributions assuming the metallacyclobutane structure are significantly narrower than experiment in both cases. A theoretical distribution that assumes 50%  $Fe^+-propene$  and 50% (ferracyclobutane $^+$ ) is given in (b), while a theoretical distribution assuming 33% ( $Co^+-propene$ ) and 67% (cobaltacyclobutane) is given in (a). Both cases yield good agreement with experiment.

propene structure was assumed. However, the calculated distribution was narrower than the experimental distribution when the metallacyclobutane structure was assumed (see Table III and Figure 9a,b). Since  $C_3H_6$  loss from both **13** and **14** in Scheme VI for  $M = Co$  and  $Fe$  are observed, loss of  $C_2H_4$  is expected to occur from **13** and **14** as well. The experimental distribution for  $C_2H_4$  loss may thus be a composite of both reaction processes outlined in Scheme V with an average kinetic energy release lying between the calculated distributions. A theoretical distribution that assumes 33% (cobalt-propene) and 67% (cobaltacyclobutane) as the product ions gives a good fit with the experimental distribution as shown in Figure 9a. For the iron system a 50/50% composition is shown to give the best fit (Figure 9b).

## Conclusion

The results of this study of the reactions of  $Co^+$  and  $Fe^+$  with cyclobutanone and 1-pentene complement the findings from previous investigations of these reactions and confirm many of the previous conclusions. For both iron and cobalt reacting with cyclobutanone, the loss of  $CO$  and  $C_3H_6$  is observed. Collision-induced dissociation of the final decomposing intermediate,  $OCM^+C_3H_6$ , indicates metallacyclobutanecarbonyl to be the structure rather than metal propenecarbonyl. Thus the  $MC_3H_6^+$  product ion formed when  $CO$  is lost is metallacyclobutane, and when  $C_3H_6$  is lost it has the cyclopropane structure for both iron and cobalt. The large kinetic energy release associated with the

Table VI. Input Parameters Used in Calculations

	Fe <sup>+</sup>	Co <sup>+</sup>			Fe <sup>+</sup> 
$\Delta H_{f,0}^\circ$ <sup>a</sup>	280.4	282.5	-19.74	2.98	268 <sup>f</sup>
$B^b$			0.190	0.148	0.173
$\sigma^c$			2	1	1
$\alpha^d$			7.26	2.85	
$\nu_i^e$			2978 (2)	3085	1296
			2933 (2)	3008	1276
			1816	2995	1229
			1479	2973	1164
			1402 (2)	2964	1143
			956	2932	1128
			850 (2)	2920	1043
			670	2891	992
			2975	2877	912
			1200	2854	875
			829	1826	861
			902	1645	840
			1332	1475	824
			1242	1460	767
			1124	1453	761
			454	1446	636
			3004	1410	553
			1209	1390	438
			1073	1380	393
			1470	1344	1447
			735		1257
			395		898
			50		556
					535

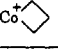
<sup>a</sup>Heat of formation at 0 K in kcal mol<sup>-1</sup>. <sup>b</sup>Rotational constants in cm<sup>-1</sup>. <sup>c</sup>Symmetry number. <sup>d</sup>Polarizability in Å<sup>3</sup>. <sup>e</sup>Vibrational frequencies in cm<sup>-1</sup>. <sup>f</sup>Rough estimate (ref 46).

loss of cyclopropane implies a barrier in the exit channel or to the reverse association of MCO<sup>+</sup> + cyclopropane.

The MC<sub>3</sub>H<sub>6</sub><sup>+</sup> ion is also produced in the ion source. Without the CO ligand, CID studies of the MC<sub>3</sub>H<sub>6</sub><sup>+</sup> ion indicate isomerization of cobaltacyclobutane occurs, at least to some extent, to form cobalt-propene, whereas the ferracyclobutane does not rearrange, in agreement with previous results.<sup>7,39</sup> However, the metastable ion kinetic energy release data for the loss of C<sub>3</sub>H<sub>6</sub> from MC<sub>3</sub>H<sub>6</sub><sup>+</sup> are identical for iron and cobalt. In this case propene is shown to be the product neutral for both iron and cobalt, indicating the barrier to rearrangement from the metallacyclobutane to the metal-propene structure is below the metal-propene dissociation limit and that the barrier to rearrangement is smaller for cobalt relative to that for iron. The relatively small statistical kinetic energy release associated with the loss of propene implies a smooth transition to products in the exit channel without a barrier.

For the 1-pentene system a bimodal distribution is observed for C<sub>3</sub>H<sub>6</sub> elimination generating both the propene and cyclopropane product neutral. The kinetic energy release distribution for the loss of cyclopropane from Co<sup>+</sup>(1-pentene) resembles that of cyclopropane elimination from Co<sup>+</sup>(cyclobutanone) almost exactly. In comparison, for the Fe<sup>+</sup>(1-pentene) system a narrower distribution than for cobalt is observed for C<sub>3</sub>H<sub>6</sub> elimination and the bimodal character observed in the cobalt system is absent. The distribution remains broad in comparison with phase space calculations for propene elimination, however, and subtraction of the latter yields a kinetic energy release distribution for the loss of cyclopropane which is similar to that observed in cyclopropane elimination from Fe<sup>+</sup>(cyclobutane). Even though a single broader distribution is observed rather than a bimodal distribution, it can be deconvoluted to separate the two contributions. The similarity of the kinetic energy release distributions compared in Figures 6 and 8 is remarkable, especially in view of the different exothermicities associated with the reactions being compared. We believe that this is due to similar *barriers* in the exit channel, with the differing reaction exothermicities being of secondary importance in determining the shape of the distributions. This observation suggests that kinetic energy release distributions may prove

Table VII. Input Parameters Used in Calculations<sup>a</sup>

	Co <sup>+</sup> 	Fe <sup>+</sup> -CO	Co <sup>+</sup> -CO	Fe <sup>+</sup> -	Co <sup>+</sup> -	Fe <sup>+</sup> -
$\Delta H_{f,0}^\circ$	274 <sup>b</sup>	227 <sup>c</sup>	224 <sup>d</sup>	260 <sup>c</sup>	255 <sup>d</sup>	252 <sup>c</sup>
$B$	0.171	0.121	0.121	0.432	0.432	0.155
$\sigma$	1	1	1	2	2	1
$\alpha$						
$\nu_i$	2895	2170	2170	3026	3026	3090
	1443 (2)	700	700	1623	1623	3013
	1001 (2)	500	500	1342	1342	2991
	2975	300	300	1023	1023	2954
	741			3103	3103	2932
	1260			949	949	2871
	1257			943	943	1650
	1219			3106	3106	1470
	926			1236	1236	1443
	1222			826	826	1420
	2893			2989	2989	1378
	2987			1444	1444	1297
	627			700	700	1171
	2952			600	600	1045
	1223			500	500	991
	749					963
	2887					920
	1447					912
	1257					578
	898					428
	556					174
	535					700
						600
						500

<sup>a</sup>Parameters as defined in Table VI. <sup>b</sup>Determined in this study. <sup>c</sup>Rough estimate (ref 46). <sup>d</sup>Reference 12b.

Table VIII. Input Parameters Used in Calculations<sup>a</sup>

	Co <sup>+</sup> -	CO	$\Delta$	#V-	C <sub>2</sub> H <sub>4</sub>
$\Delta H_{f,0}^\circ$	247 <sup>b</sup>	-27.199	16.84	8.26	14.515
$B$	0.152	1.931	0.586	0.506	1.588
$\sigma$	1	1	6	1	4
$\alpha$	1.95	5.36	5.78	4.26	
$\nu_i$	3090	2170	3038	3090	3026
	3013		1479	3013	1623
	2991		1188	2991	1342
	2954		1070	2954	1023
	2932		3103	2932	3103
	2871		854	2871	1236
	1650		3025 (2)	1650	949
	1470		1438 (2)	1470	943
	1443		1029 (2)	1443	3106
	1420		866 (2)	1420	826
	1378		3082 (2)	1378	2989
	1297		1188 (2)	1297	1444
	1171		739 (2)	1171	
	1045		1126	1045	
	963			991	
	920			963	
	912			920	
	578			912	
	428			578	
	174			428	
	991			174	
	700				
	600				
	500				

<sup>a</sup>Parameters as defined in Table VI. <sup>b</sup>Reference 12b.

to be quite useful in identifying specific reaction mechanisms on type II surfaces.

**Acknowledgment.** The support of the National Science Foundation under Grant CHE85-12711 (MTB) and Grant CHE87-11567 (JLB) is gratefully acknowledged. J.L.B. also acknowledges support from the Petroleum Research Fund administered by the American Chemical Society.

#### Appendix A

The model for statistical phase space calculations has been previously outlined.<sup>12b</sup> Here the parameters used in the calcu-

lations are summarized and the thermochemistry involved is discussed.

In order to calculate the kinetic energy distributions, structures and vibrational frequencies for the various species are required. These were taken from the literature where possible, or estimated from literature values of similar species.<sup>45</sup> The details of the kinetic energy distributions were found to vary only weakly with structure or vibrational frequencies over the entire physically reasonable range for these quantities. The distributions were strongly dependent on the total energy available to the dissociating complex, and hence in our model to the  $\Delta H^\circ$  of reaction. Often all heats of formation of products and reactants were well known except one, the organometallic product ion. The heats of formation for  $\text{Co}(\text{propene})^+$ ,  $\text{Co}(\text{carbonyl})^+$ , and  $\text{Co}(\text{ethylene})^+$  have been previously determined.<sup>12b</sup> The bond energies for the corresponding

iron species have also been determined.<sup>46</sup> The heats of formation for cobalt- and ferracyclobutane were determined in this study and are consistent with the heats of formation inferred from ligand displacement reactions.<sup>38</sup> These heats of formation were consistently used throughout the calculations and are summarized along with the other parameters in Table VI-VIII.

**Registry No.**  $\text{Fe}^+$ , 14067-02-8;  $\text{Co}^+$ , 16610-75-6;  $\overline{\text{CH}_2\text{CH}_2\text{CH}_2\text{C}(\text{O})}$ , 1191-95-3;  $\text{CH}_2=\text{CHCH}_2\text{CH}_2\text{CH}_3$ , 109-67-1.

(46) Heats of formation for  $\text{Fe}(\text{propene})^+$ ,  $\text{Fe}(\text{carbonyl})^+$ ,  $\text{Fe}(\text{ethylene})^+$ , and for the ferracyclobutane ion were obtained by fitting the theoretical kinetic energy release distributions to the experimental distributions in all cases. A distinctive high-energy tail is observed for the experimental distributions which is not reproduced theoretically (see Figure 3b). In contrast, nearly exact fits were found for all the cobalt systems studied (see Figure 3a and ref 12b). The bond energies obtained by fitting the low-energy part of the distributions appears to be giving low bond energy values for iron relative to the corresponding cobalt species and relative to heats of formation inferred from ligand displacement reactions. As a result, the bond energies for the iron system are rough estimates. We are currently looking into the origin of these effects and will publish our results in a future publication.

(45) (a) Shimanouchi, T. *Table of Molecular Vibrational Frequencies*, Consolidated, Vol. I; National Bureau of Standards: Washington, DC, 1972. (b) Sverdlov, L. M.; Kovner, M. A.; Krainov, E. P. *Vibrational Spectra of Polyatomic Molecules*; Wiley: New York, 1970.

## Photophysical Recognition of Chiral Surfaces

David Avnir,\* Edna Wellner, and Michael Ottolenghi\*

*Contribution from the Institute of Chemistry and the F. Haber Research Center for Molecular Dynamics, The Hebrew University of Jerusalem, Jerusalem 91904, Israel. Received June 8, 1988*

**Abstract:** We report that *R* and *S* quenchers [(*R*)-(+)- and (*S*)-(-)-*N,N*-dimethyl-1-phenethylamine, RQ and SQ] recognize differently an *R* excited-state chiral surface (silica derivatized with (*R*)-(-)-1,1-bisnaphthyl-2,2'-dihydrogen phosphate, RS). This is revealed by a  $\sim 30\%$  difference in Stern-Volmer constants between RQ/RS and SQ/RS. A similar recognition difference was obtained between these quenchers and the corresponding *S*-(+)- surface. The surface derivatization enhances the chiral recognition; in solution, no difference between the constants was observed. It is suggested that what we believe to be the first observation of a photophysical recognition of a chiral surface can be explained in terms of an increase in the relative weight of an exciplex formation (over ion-pair formation) quenching route and in terms of the decrease in the dimensionality of the quenching process.

### Background

The crucial role of the geometry of the environment on reaction pathways in heterogeneous (photo)chemistry is now well established.<sup>1</sup> In surface photochemistry, the main relevant surface geometry parameters are the average pore size,<sup>2</sup> the degree of surface irregularity as determined through its fractal dimension,<sup>3</sup> and the geometry of the adsorbate-adsorbent interactions.<sup>4</sup> Here we wish to report that the *chirality* of a surface may affect the pathway of its photophysical interactions: in particular, that *R* and *S* quenchers recognize differently an excited state of an *R*-derivatized chiral surface, and that the same recognition difference exists between this pair of quenchers and an *S* chiral surface.

Chiral recognition in photoprocesses<sup>5</sup> carried out in chiral environments has been reported in several cases (e.g., crown ethers,<sup>6a</sup>

dextrin,<sup>6b</sup> chiral crystals,<sup>6c</sup> enzyme<sup>6d</sup>), but we are unaware of any photochemical recognition of a chiral surface. Horner and Klaus<sup>7</sup> derivatized the surface of silica with a chiral photosensitizer but observed no effect on the *cis*-*trans* chiral photoisomerization of 1,2-diphenylcyclopropane. In spite of this specific unsuccessful case, the idea of a photophysical chiral surface recognition seemed to us feasible, not only in view of the observations in ref 6, but mainly because of the great progress and success in chromatographic separations of enantiomers.<sup>8,9</sup> These are clearly indicative of substantial differences in the interactions of two enantiomers with a chiral surface. For our purpose (see below) we notice, in particular, that the enantiomers of chiral amine compounds and of binaphthyl derivatives are separable chromatographically.<sup>8,9</sup> Consequently, from the various chiral photoprocesses reported for *homogeneous* solutions,<sup>5</sup> we chose to concentrate on the observation of Irie et al.<sup>10</sup> that the quenching of (unsubstituted)

(1) (a) *Photochemistry on Solid Surfaces*; Anpo, M., Matsuura, T., Eds.; Elsevier: Amsterdam, 1989. (b) Turro, N. J. *Pure Appl. Chem.* **1986**, *58*, 1219.

(2) E.g. (a) Turro, N. J.; Chen, C. C.; Mahler, W. *J. Am. Chem. Soc.* **1984**, *106*, 5022. (b) Wellner, E.; Rojanski, D.; Ottolenghi, M.; Huppert, D.; Avnir, D. *J. Am. Chem. Soc.* **1987**, *109*, 575. (c) Pines, D.; Huppert, D. *J. Phys. Chem.* **1987**, *91*, 6569. Drake, J. M.; Levitz, P.; Turro, N. J.; Nitsche, K. S.; Cassidy, K. F. *J. Phys. Chem.* **1988**, *92*, 4680.

(3) (a) Vlachopoulos, N.; Liska, P.; Augustinski, J.; Grätzel, M. *J. Am. Chem. Soc.* **1988**, *110*, 1216. (b) Avnir, D. *J. Am. Chem. Soc.* **1987**, *109*, 2931. (c) Seri-Levy, A.; Samuel, J.; Farin, D.; Avnir, D. In ref 1a, p 353.

(4) Levy, A.; Avnir, D.; Ottolenghi, M. *Chem. Phys. Lett.* **1985**, *122*, 233.

(5) Rau, H. *Chem. Rev.* **1983**, *83*, 535.

(6) (a) Tundo, P.; Fendler, J. H. *J. Am. Chem. Soc.* **1980**, *102*, 1760. (b) Ueno, A.; Saka, R.; Takahashi, K.; Osa, T. *Heterocycles* **1981**, *15*, 671. Kano, K.; Matsumoto, H.; Hashimoto, S.; Sisido, M.; Imanishi, Y. *J. Am. Chem. Soc.* **1985**, *107*, 6117. (c) Weis, R. M.; McConnell, H. M. *Nature (London)* **1984**, *310*, 47. (d) Gafni, A. *J. Am. Chem. Soc.* **1980**, *102*, 7367.

(7) Horner, L.; Klaus, J. *Justus Liebigs Ann. Chem.* **1981**, 792.

(8) E.g.: Roumeliotis, P.; Unger, K. K.; Kurganov, A. A.; Davankov, V. A. *J. Chromatogr.* **1983**, *225*, 51. For a recent review, see: Kinkel, J. N.; Fraenkel, W.; Blaschke, G. *Kontakte (Darmstadt)* **1987**, (1), 3.

(9) Okamoto, Y.; Honda, S.; Okamoto, I.; Yuki, H.; Murata, S.; Noyori, R.; Takaya, H. *J. Am. Chem. Soc.* **1981**, *103*, 6971. Pirkle, W. H.; Reno, D. S. *J. Am. Chem. Soc.* **1987**, *109*, 7189.